Proc. of the European Safety and Reliability Conference (ESREL 2026)
Edited by José C. Matos, Paulo B. Lourenço, Michael Beer, Daniel Oliveira, Edoardo Patelli, Hélder S. Sousa, Rui A. Silva, Monica Santamaria and Chiara Turco
© 2026 ESREL 2026 Organizers. *Published by* Research Publishing, Singapore.
ISBN: 978-981-94-6718-1 | doi: 10.3850/ESREL2026061419_esrel26-p26262-cd

Reliability Assessment Method for Motors under Extreme Environments Based on Competing Failure Modeling

Xuetong Ku
School of Reliability and Systems Engineering, Beihang University, China. E-mail: ZY2414117@buaa.edu.cn

Jun Yao
School of Reliability and Systems Engineering, Beihang University, China. E-mail: yao2jun1@sina.com

Guo Chen
AECC Sichuan Gas Turbine Establishment, China. E-mail: jia187590chen@2925.com

Huan Lu
AECC Sichuan Gas Turbine Establishment, China. E mail: jia187590huan@2925.com

Chunping Hu
China Aviation Engine Nanjing Aer-Propulsion Co. Ltd, China. Email: ja187590hu@2925.com

Sa Wu
School of Reliability and Systems Engineering, Beihang University, China. E-mail: wusa@buaa.edu.cn

Xiaogang Li
School of Reliability and Systems Engineering, Beihang University, China. E-mail: Ixg@buaa.edu.cn

Xiaohui Wang
School of Reliability and Systems Engineering, Beihang University, China. E-mail: xiaohuiw@buaa.edu.cn

Xiaohong Wang
School of Reliability and Systems Engineering, Beihang University, China. E-mail: wxhong @ buaa.edu.cn

Under certain special environmental conditions, the failure mechanisms of motor systems often exhibit the coexistence of degradation-induced failures and sudden shock-induced failures, making traditional reliability analysis methods based on a single failure mode inadequate for accurately characterizing such complex failure behaviors. To address this issue, this paper proposes a motor reliability assessment method based on competing failure modeling. First, by analyzing lifetime data of motors operating under special environments such as low temperature and icing/freezing rain, marginal distribution models for degradation failures and shock failures are established, respectively. Subsequently, a Copula function is introduced to describe the statistical dependence between the two failure modes, and a degradation–shock competing failure model is constructed to capture the joint failure behavior of the motor system. Finally, combined with simulation data, the variations in reliability under different environmental stress levels are evaluated. The results demonstrate that, compared with single-failure-mode approaches, the proposed method yields reliability predictions that are closer to actual conditions, effectively reflecting the coupled effects of multiple failure mechanisms in special environments and significantly improving the accuracy and applicability of reliability assessment. The proposed approach provides a new modeling framework and theoretical reference for reliability design and lifetime prediction of motor systems under complex service conditions.

Keywords: Motor reliability, Competing failure model, Degradation failure, Shock-induced failure, Copula function, Special environments.

1. Introduction

Under polar and marine environments, equipment systems are exposed to the combined effects of multiple factors, including low temperatures, icing, strong winds, salt spray, and severe humidity fluctuations. Consequently, their performance degradation behaviours and failure mechanisms differ significantly from those under conventional operating conditions(Gao et al. 2019; Su et al. 2024). Low temperatures reduce the plasticity and fracture toughness of metallic materials, leading to embrittlement and crack propagation; high-humidity and salt-spray environments readily induce electrical corrosion and insulation degradation; and temperature cycling may cause thermal stress concentration and solder joint fatigue (Wileman et al. 2021). The long-term superposition of multiple environmental stresses causes the reliability evolution of equipment to exhibit characteristics of multi-mechanism coupling and pronounced uncertainty.

Taking polar marine equipment as a representative example, startup reliability after long-term storage is a critical indicator, as environmental factors can induce lubricant degradation and instantaneous damage. During operation, motors face not only continuous performance degradation (Lang et al. 2025), but also sudden failures caused by random shocks, such as ice impacts and wave-induced vibrations (Huang et al. 2023). The failure process is essentially characterized by the competition and coexistence of "slow degradation" and "random shocks."

However, existing methods typically assume a single failure mechanism(Muhammad et al. 2024). In degradation modeling, researchers often utilize stochastic processes, such as the Gamma process and its variants(Leadbetter et al. 2024; Castro and Landesa 2024) , while shock modeling focuses on the characterization of extreme shocks and stochastic thresholds(Dshalalow and White 2022; Shamstabar et al. 2024; Mohtashami-Borzadaran et al. 2021). However, given the multi-mechanism coexistence and small sample data constraints in polar environments, traditional models struggle to accurately capture failure characteristics, often leading to prediction bias.

Against this background, this paper focuses on marine machinery motors operating in polar environments. Aiming at the failure characteristics arising from the concurrent effects of degradation and random shocks, competing failure theory is introduced to develop a reliability modeling and assessment framework capable of simultaneously describing performance degradation evolution and sudden shock effects. The proposed approach provides theoretical foundations and engineering support for the analysis of cold-resistance validation test data, lifetime prediction, and reliability assessment of polar equipment.

2. Basic Structure and Failure Analysis of Marine Deck Motors

2.1. *Basic Structure of Deck Motors*

Electric motors used in marine deck machinery serve as the power source for deck equipment, providing the driving force required for deck machinery to perform its intended functions. Marine deck machinery is mainly composed of lifting and hauling equipment, such as windlasses, winches, cranes, and gangway winches.

Deck motors for marine lifting applications mainly consist of a stator (including the housing, stator core, and armature windings), a rotor (including the shaft and rotor core), as well as end covers, position sensors, and other components. The basic structure of a typical deck motor is illustrated in Fig. 1 and Fig. 2.

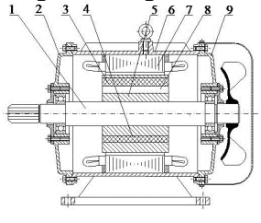


Fig. 1 Basic structure of a marine deck motor.

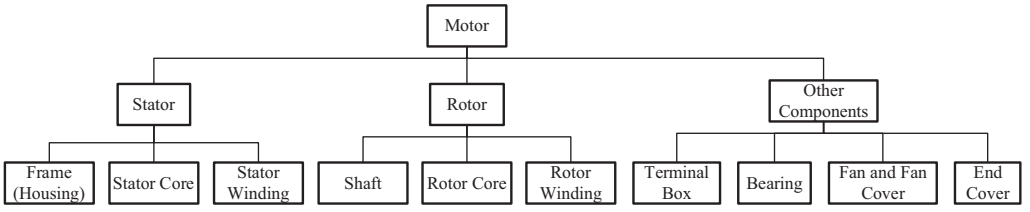


Fig. 2 Main components of the motor assembly

Deck machinery mostly uses three-phase AC induction motors. When stator windings are powered, they create a synchronous-speed rotating magnetic field. This field cuts rotor conductors to induce rotor current; the current interacts with the magnetic field to produce torque, spinning the rotor and converting electricity to mechanical energy.

The stator is built with laminated high-permeability silicon steel core embedded with three-phase armature windings to generate the rotating magnetic field. Its windings adopt moisture and salt-spray resistant F/H-class insulation, enabling stable long-term operation in humid marine conditions.

2.2. *Failure Mode Analysis of Deck Motors*

Marine deck machinery motors operating for extended periods under polar multi-stress coupled environments are simultaneously subjected to multiple environmental stresses, including low temperature, high humidity, vibration, and salt-spray corrosion. These factors inevitably lead to degradation in component performance and a decline in overall reliability. The operating environment of deck machinery motors is characterized by large fluctuations in temperature and humidity as well as strong corrosiveness. Specifically, the typical operating temperature range is from −25 °C to 45 °C, which may rise to 60 °C under special conditions. The ambient relative humidity can reach up to 95%, and the motors may be exposed to condensation, salt spray, oil mist, mold, as well as seawater corrosion and immersion. Furthermore, the shocks and vibrations induced by vessel inclination and rolling, combined with continuous erosion from high-humidity and high-salt environments, further accelerate the degradation process of the motors.

Under the combined influence of the aforementioned environmental stresses, various failure modes may occur, including phase-to-phase or phase-to-ground short circuits of windings, inter-turn short circuits, bearing damage or lubrication failure, corrosion of the motor frame or shaft, and stator–rotor rubbing, as summarized in Table 1.

Table 1. Failure Mode Analysis of the Motor.

Components	Failure Mode	Failure Mechanism	Sensitive Stress	Severity/Impact
Stator Windings	Insulation aging, short circuit	Chemical/Thermal Aging	Temp, Humidity, Salt spray	Severe; leading to functional failure
Bearings	Fracture, lubrication failure, inflexible rotation	Fatigue, Wear, Overstress	Vibration, Shock, Temp	General/Severe; accelerated by lubricant oxidation
Rotor & Shaft	Corrosion, stator-rotor rubbing	Corrosion, Mechanical Wear	Seawater, Humidity, Salt spray	General; impact depends on operation status
Core/Housing	Magnetic degradation, loosening, oil leakage	Corrosion, Fatigue	Salt spray, Vibration	General; minimal impact with protection

3. Competing Failure Reliability Analysis

3.1. *Random Shock Models*

Sudden failures, triggered by external shocks, occur independently of long-term degradation. Characterized by randomness and instantaneity, they typically manifest as component failure from mechanical impacts, power surges, or electrical overloads. Common modeling approaches include cumulative, δ -model, and extreme shock models, with selection depending on specific failure mechanisms and data characteristics.

Motor FMEA indicates abrupt motor failures are mainly caused by overstress shocks stemming from bearing damage under excessive external loads. This study therefore employs the extreme shock model to describe sudden motor system failures.

Distinct from cumulative shock models, the extreme shock model centers on individual random shocks. An extreme shock has an excessively large amplitude surpassing the system critical threshold and triggers instantaneous failure, such as diode breakdown when subjected to overvoltage or overcurrent beyond its rated capacity.

In the extreme shock process, the shock amplitude is denoted by W_i, and the hard failure threshold of the extreme shock process is denoted by D. When the amplitude of any shock exceeds the hard failure threshold, the system experiences shock-induced hard failure. The arrival process of shocks is assumed to be a homogeneous Poisson process with parameter θ. Then, the probability that $N(t)$ shocks occur in the interval [0,t] is given by:

$$P(N(t)=n)=\exp(-\lambda t)\frac{(\lambda t)^n}{n!}$$

where $N(t)$ represents the number of shocks, λ is the arrival rate of the shock process, and $n=0,1,2,\ldots$. It is generally assumed that the shock amplitudes are independent and identically distributed, denoted as $W_i \sim N(\mu_W,\sigma_W^2)$. The probability that the component does not fail when subjected to a single shock is given by:

$$P(W_i<D)=\Phi\left(\frac{D-\mu_W}{\sigma_W}\right)$$

where D is the hard failure threshold, and $\Phi(\cdot)$ is the cumulative distribution function of a standard normal random variable. The probability that the component remains reliable under extreme shock loading is:

$$R(t)=\sum_{n=0}^{\infty}P\left(N(t)=n,\bigcap_{i=1}^{n}(W_i<D)\right)=\sum_{n=0}^{\infty}P(N(t)=n)\cdot\prod_{i=1}^{n}P(W_i<D)$$

3.2. *Degradation Process Models*

Key performance degradation differs by equipment type with unique statistical features and stochastic trends, which should be modeled via stochastic processes matching degradation mechanisms and measured data. Wiener and Gamma processes are commonly adopted to model degradation of deck machinery motors under polar multi-stress conditions.

Failure analysis reveals armature winding aging and corrosion as the main degradation modes of these motors. Such deterioration evolves continuously with random fluctuations instead of strictly monotonic growth. Accordingly, this study chooses the Wiener process to fit motor degradation paths, since it can well describe both the deterministic trend and random volatility of insulation aging.

The Wiener process is a class of stochastic processes with continuous trajectories and independent increments, and it is commonly used to describe degradation behaviors that exhibit both deterministic trends and random fluctuations. Assuming that the product performance degradation amount $Y(t)$ follows a Wiener degradation process, its mathematical form can be expressed as:

$$Y(t)=Y(0)+\mu A(t)+\sigma B(\Lambda(t))$$

where μ is the drift parameter, $\sigma(\sigma>0)$ is the diffusion parameter, $\Lambda(t)$ is a function of time, and $B(\Lambda(t))$ denotes standard Brownian motion related to the function of time. The initial degradation amount is assumed to be $Y(0)=0$. For a Wiener process, the degradation increment $\Delta Y(t)=Y(t+\Delta t)-Y(t)$ follows a normal

distribution $N\left(\mu\Delta\Lambda(t),\sigma^2\Delta\Lambda(t)\right)$, where $\Delta\Lambda(t)=\Lambda(t+\Delta t)-\Lambda(t)$. The probability density function of the degradation amount $Y(t)$ is given by:

$$f(Y)=\frac{1}{\sqrt{2\pi\sigma^2\Lambda(t)}}\exp\left\{-\frac{(Y-\mu\Lambda(t))^2}{2\sigma^2\Lambda(t)}\right\}-\exp\left(\frac{2\mu D}{\sigma^2}\right)\exp\left[-\frac{(Y-2D-\mu t)^2}{2\sigma^2\Lambda(t)}\right]$$

When *s*=0, the mathematical expectation and variance of the Wiener process are respectively:

$$E(Y(t))=0$$

$$Var(Y(t))=E(Y(t)^2)-E^2(Y(t))=t$$

When the product degradation follows a Wiener process, the failure threshold of the performance parameter is defined as D, and the product lifetime is denoted by T. $T=\inf\{t\mid Y(t)\geq D\}$ represents the first passage time when $Y(t)$ first crosses D. According to the statistical properties of the Wiener process, the lifetime T follows an Inverse Gaussian distribution, and the reliability function of the product is given by:

$$R(t)=\Phi\left[\frac{D-\mu\Lambda(t)}{\sigma\sqrt{\Lambda(t)}}\right]-\exp\left(\frac{2\mu D}{\sigma^2}\right)\Phi\left[-\frac{D+\mu\Lambda(t)}{\sigma\sqrt{\Lambda(t)}}\right]$$

3.3. *Competing Failure System Reliability Model*

Based on the degradation modeling of stator insulation windings and the sudden/shock failure modeling of bearings, a unified competing failure model integrating the two failure mechanisms is further established to achieve a quantitative characterization of the overall failure behavior of the motor under polar environmental conditions.

A significant statistical dependence exists between these mechanisms, as environmental stressors and bearing shock events can accelerate winding insulation aging. To capture this interaction, a Copula function is employed to construct the joint distribution from the marginal distributions of degradation failure time T_D and sudden failure time T_I:

$$H(t_D,t_I)=C(F_D(t_D),F_I(t_I);\theta)$$

An appropriate Copula (such as Gumbel、Clayton、or Frank Copula) is selected according to the dependence structure characteristics, thereby enabling a reasonable description of different tail dependencies and improving the joint failure behavior modeling of key motor components.

A Copula function is a linking function that connects the joint distribution function $F(x_1,x_2,\cdots,x_N)$ of a random vector $X_1,X_2,\cdots,X_N$ with its corresponding marginal distribution functions $F(x_1),F(x_2),\cdots,F(x_N)$, as shown in the equation. When $F(x_1),F(x_2),\cdots,F(x_N)$ is continuous, the Copula function is uniquely determined.

$$F(x_1,x_2,\cdots,x_n)=C(F_1(x_1),F_2(x_2),\cdots,F_N(x_N))$$

Copula functions can be used to measure the dependence among continuous random variables. Consider two continuous random variables (X,Y) with marginal distribution functions $F(x)$ and $G(y)$, and joint distribution function $C(u,v)$. τ,ρ,λ denote the Kendall rank correlation coefficient, the Spearman rank correlation coefficient, and the tail dependence coefficient of the random variables, respectively. Their relationships are given by:

$$\tau=4\int_0^1\int_0^1 C(u,v)\mathrm{d}C(u,v)-1$$

$$\rho=12\int_0^1\int_0^1 uv\mathrm{d}C(u,v)-3$$

$$\begin{cases}\lambda^{\mathrm{up}}=\lim\limits_{u\to1}\dfrac{1-2u+C(u,v)}{1-u}\\ \lambda^{\mathrm{lo}}=\lim\limits_{u\to0^+}\dfrac{C(u,v)}{u}\end{cases}$$

where:

$$U=F(x)\sim U(0,1);$$

$$V=G(y)\sim U(0,1);$$

$$C(1-u,1-v)=P(U>u,V>v)=1-u-v+C(u,v)$$

There are many types of Copula functions, and different Copula functions are used to characterize different dependence patterns. With respect to Copula selection, the Akaike Information Criterion (AIC) is commonly adopted, which is applicable to Copula models estimated using the maximum likelihood method.

$$\mathrm{AIC}=-2\ln(\mathrm{MLE})+2k$$

$$C_{opt}=\arg\min(\mathrm{AIC})$$

Here, k is the number of unknown parameters, and the Copula with the smallest AIC is selected as the optimal one.

Sklar's theorem enables constructing multivariate joint distributions using a specified Copula. Archimedean Copulas, including Gumbel, Clayton and Frank types, are widely used due to their simple structure and great flexibility.

For polar motors, one failure mode (e.g., bearing shock) tends to induce or expedite another (e.g., winding insulation failure), presenting obvious upper tail dependence matching the property of the Gumbel Copula. Thus this paper uses the Gumbel Copula to describe such correlation.

The expression of the two-dimensional Gumbel Copula function is given by:

$$C(u,v;a)=\exp\left\{-[(-\ln u)^{\alpha}+(-\ln v)^{\alpha}]^{\frac{1}{\alpha}}\right\}$$

The corresponding probability density function is:

$$c(u,v)=\frac{C(u,v)(\ln u\cdot\ln v)^{\alpha-1}}{uv[(-\ln u)^{\alpha}+(-\ln v)^{\alpha}]^{2-\frac{1}{\alpha}}}\left\{[(-\ln u)^{\alpha}+(-\ln v)^{\alpha}]^{2-\frac{1}{\alpha}}+\alpha-1\right\}$$

where α is the dependence parameter and $\alpha\in[1,+\infty)$. When $\alpha=1$, the random variables u and v are independent; when $\alpha\to+\infty$, the random variables u and v tend to be completely dependent. The relationship between the Kendall rank correlation coefficient τ and the dependence parameter α is given by:

$$\tau=1-\frac{1}{\alpha}$$

4. Simulation Case Study

In this section, numerical simulation experiments are conducted to verify the effectiveness of the proposed model. It is assumed that a certain type of motor used in marine deck machinery undergoes 60 months of storage. During the storage period, periodic inspections are carried out every 10 days per month, and the reliability requirement is that the reliability at 40 months of service should not be less than 0.7. The test data include sudden failure data represented by the shock intensities experienced by the bearings and degradation data represented by the degradation values of the insulation windings.

The assumptions for sudden failure are as follows: during the storage period, the number of random shocks experienced by the bearings follows a Poisson process with intensity λ. The bearing fails immediately only when the intensity W_i of a shock exceeds the critical threshold D of the bearing.

Shock intensity distribution: it is assumed that the intensity W_i of each shock follows an exponential distribution with mean μ.

Reliability function: the probability that the bearing does not fail within time t, which is equivalent to the probability that none of the n shocks occurring within time t exceeds the threshold D.

$$R_s(t)=\sum_{n=0}^{\infty}\frac{(\lambda t)^n e^{-\lambda t}}{n!}[P(X<D)]^n=e^{-\lambda t[1-P(X<D)]}$$

The degradation assumptions are as follows: the aging of the motor insulation windings is considered a continuous degradation process, and a Wiener process is used to describe its degradation trajectory $Y(t)$:

$$Y(t)=\mu t+\sigma B(t)$$

Failure criterion: when the degradation amount $Y(t)$ reaches the prescribed critical threshold L, the winding fails.

Its lifetime T_d follows an Inverse Gaussian Distribution, and the corresponding reliability function $R_d(t)$ is given by:

$$R_d(t)=\Phi\left(\frac{L-\mu t}{\sigma\sqrt{t}}\right)-\exp\left(\frac{2\mu L}{\sigma^2}\right)\Phi\left(-\frac{L+\mu t}{\sigma\sqrt{t}}\right)$$

where $\Phi(\cdot)$ denotes the cumulative distribution function of the standard normal distribution.

Integrated failure modeling: a Copula-based competing failure model is adopted. The commonly used Gumbel Copula is selected (which is suitable for describing tail dependence, i.e., when one component fails rapidly, the other also tends to fail):

$$C(u,v)=\exp\left(-[(-\ln u)^{\theta}+(-\ln v)^{\theta}]^{1/\theta}\right)$$

where $\theta\in[1,\infty)$ is the dependence parameter. When $\theta=1$, the two failure processes are completely independent.

Overall system reliability function

The overall reliability $R_{sys}(t)$ of the motor is defined as the joint probability that both the bearing and the winding do not fail:

$$R_{sys}(t) = P(T_s > t, T_d > t) = C(R_s(t), R_d(t))$$

Substituting the specific Copula form yields:

$$R_{sys}(t) = \exp\left(-\left[(-\ln R_s(t))^{\theta} + (-\ln R_d(t))^{\theta}\right]^{1/\theta}\right)$$

Specific parameter settings:

Parameter initialization:

Shock: $\lambda = 0.08$ occurrences/month, $D = 500$ units, $X \sim Exp(200)$.

Degradation: $\mu = 1$ units/month, $\sigma = 0.9$, $L = 50$ units.

Dependence: $\theta = 2$.

Trajectory generation: Monte Carlo simulation is used to generate 1000 sets of degradation trajectories and random shock sequences.

Lifetime calculation: for each sample, the minimum value of T_s and T_d is recorded as the system lifetime of the motor.

The resulting reliability function is shown in Fig. 3.

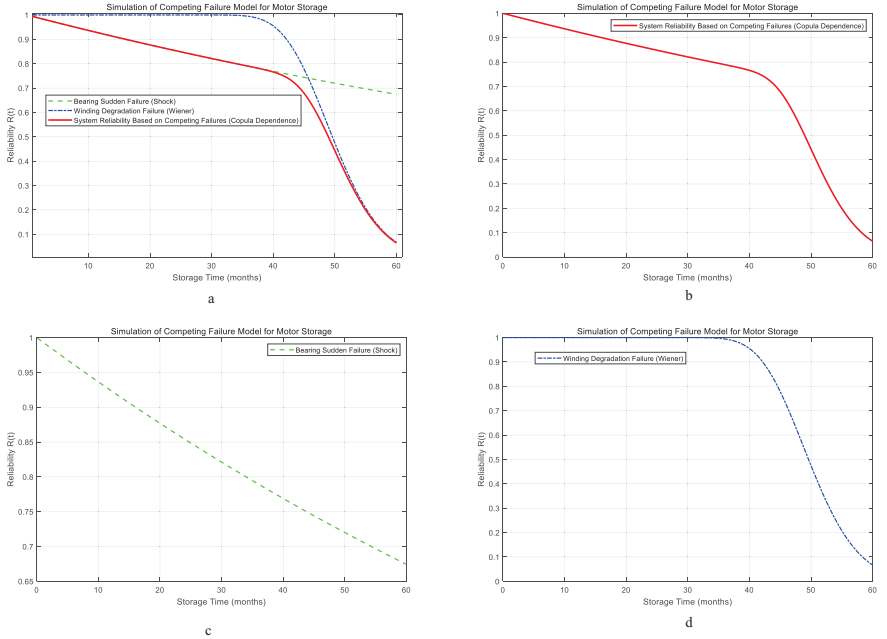


Fig. 3. Simulation of Competing Failure Model for Motor Storage

From the simulation curves of the three models (sudden failure, slow degradation failure, and Copula-based competing failure), the stage-wise influence of different failure modes on system reliability is clearly illustrated.

For this competing-failure system, reliability falls to 0.7 at roughly 44 months. Within the first 36 months of storage, sudden failure governs system failure: the slow degradation curve stays near 1.0 with nearly no influence on reliability, while the gradual decline of the sudden failure curve dictates the overall system reliability.

After 36 months, slow degradation becomes the primary failure mode. Its curve drops rapidly and dominates total reliability decline, even as sudden failure continues to decrease moderately.

The competing-failure model outperforms single-failure alternatives for motor storage reliability assessment. The green sudden-failure curve declines steadily over the whole storage period, whereas the blue degradation curve remains flat initially before steeply decreasing. The red competing-failure curve integrates both tendencies, matching real-world coexistence of sudden and degradation failures.

In the first 36 months, the red curve decreases alongside the green one, eliminating early risk underestimation seen in the single degradation

model. Post 36 months, it falls sharply with the blue curve and avoids overestimating long-term reliability from the single sudden-failure model, enabling accurate full-lifetime description.

Furthermore, the Copula-derived red curve accounts for coupling between the two failure modes instead of simple independent superposition, quantifying their correlation and more faithfully reflecting actual system failure characteristics.

5. Conclusions

Motors under special environments usually show both degradation and sudden failures under multi-stress coupling. Traditional single-failure reliability methods cannot accurately evaluate their reliability. This paper presents a motor reliability assessment approach based on competing failure modeling, which characterizes both performance degradation and sudden failure mechanisms, allowing comprehensive reliability evaluation under special environments.

(i) The proposed method is suitable for motors under complex multi-stress environments with multiple failure modes, providing a unified framework for reliability prediction and assessment.

(ii) The competing failure framework overcomes the limitations of traditional methods in describing multiple failure mechanisms, improving the rationality of reliability prediction.

(iii) Simulation cases verify the feasibility and engineering applicability of the method, which can effectively predict motor reliability under special environments and provide a technical approach for reliability evaluation under multi-stress coupling.

Although the competing failure model is superior to traditional single-failure methods, this study still has limitations. On the one hand, the extreme shock model does not fully consider cumulative shock damage. On the other hand, the linear Wiener model cannot describe nonlinear degradation. Future work will introduce cumulative shock effects and nonlinear degradation to further improve the robustness and applicability of the method in complex engineering scenarios.

References

Castro, Inma T., and L. Landesa. 2024. ‘A Dependent Complex Degrading System with Non-Periodic Inspection Times’. arXiv:2401.09141. Preprint, arXiv, January 17.

Dshalalow, Jewgeni H., and Ryan T. White. 2022. ‘Fluctuation Analysis of a Soft-Extreme Shock Reliability Model’. Mathematics 10 (18): 3312.

Gao, Hongda, Lirong Cui, and Qingan Qiu. 2019. ‘Reliability Modeling for Degradation-Shock Dependence Systems with Multiple Species of Shocks’. Reliability Engineering & System Safety 185 (May): 133–43.

Huang, Yating, Songsong Yu, Tai An, Guojun Wang, and Dayong Zhang. 2023. ‘Investigating the Ice-Induced Fatigue Damage of Offshore Structures by Field Observations’. Journal of Marine Science and Engineering 11 (10): 1844.

Lang, Fengyong, Zhenrui Zhou, Jia Liu, Meng Cui, and Zhongqing Zhang. 2025. ‘Review on the Impact of Marine Environment on the Reliability of Electronic Packaging Materials’. Frontiers in Materials 12 (April): 1584349.

Leadbetter, Ryan, Gabriel Gonzalez Caceres, and Aloke Phatak. 2024. ‘Bayesian Hierarchical Modelling of Noisy Gamma Processes: Model Formulation, Identifiability, Model Fitting, and Extensions to Unit-to-Unit Variability’. arXiv:2406.11216. Preprint, arXiv, June 17.

Mohtashami-Borzadaran, H. A., H. Jabbari, and M. Amini. 2021. ‘BIVARIATE MARSHALL–OLKIN EXPONENTIAL SHOCK MODEL’. Probability in the Engineering and Informational Sciences 35 (3): 745–65.

Muhammad, Isyaku, Mustapha Muhammad, Baohua Wang, Wang Chen, Badamasi Abba, and Mustapha Mukhtar Usman. 2024. ‘Reliability Analysis for Degradation-Shock Processes with State-Varying Degradation Patterns Using Approximate Bayesian Computation (ABC) for Parameter Estimation’. Symmetry 16 (10): 1364.

Shamstabar, Yousof, Neda Ebrahimmagham, and Hamid Shahriari. 2024. ‘Monitoring Reliability of a System with Random Failure Threshold under Extreme Shocks’. Reliability Engineering & System Safety 245 (May): 109973.

Su, Zhongji, Zexi Hua, Die Hu, and Mingjing Zhao. 2024. ‘Research on Equipment Reliability Modeling and Periodic Maintenance Strategies in Dynamic Environment’. Eksploatacja i Niezawodność – Maintenance and Reliability 27 (1).

Wileman, Andrew, Suresh Perinpanayagam, and Sohaib Aslam. 2021. ‘Physics of Failure (PoF) Based Lifetime Prediction of Power Electronics at the Printed Circuit Board Level’. Applied Sciences 11 (6): 2679.